

# Efficacy and predictive biomarkers of immunotherapy in Epstein-Barr virus-associated gastric cancer

Yuezhong Bai,<sup>1</sup> Tong Xie,<sup>1</sup> Zhenghang Wang,<sup>1</sup> Shuang Tong,<sup>2</sup> Xiaochen Zhao,<sup>2</sup> Feilong Zhao,<sup>2</sup> Jinping Cai,<sup>2</sup> Xiaofan Wei,<sup>3</sup> Zhi Peng,<sup>1</sup> Lin Shen <sup>1</sup>

**To cite:** Bai Y, Xie T, Wang Z, *et al.* Efficacy and predictive biomarkers of immunotherapy in Epstein-Barr virus-associated gastric cancer. *Journal for ImmunoTherapy of Cancer* 2022;**10**:e004080. doi:10.1136/jitc-2021-004080

► Additional supplemental material is published online only. To view, please visit the journal online (<http://dx.doi.org/10.1136/jitc-2021-004080>).

YB and TX contributed equally.

Accepted 31 January 2022



© Author(s) (or their employer(s)) 2022. Re-use permitted under CC BY-NC. No commercial re-use. See rights and permissions. Published by BMJ.

<sup>1</sup>Department of Gastrointestinal Oncology, Key Laboratory of Carcinogenesis and Translational Research (Ministry of Education), Peking University Cancer Hospital & Institute, Beijing, China

<sup>2</sup>Medical Affairs, 3D Medicines, Inc, Shanghai, China

<sup>3</sup>Department of Human Anatomy, Histology and Embryology, School of Basic Medical Sciences, Peking University Health Science Center, Beijing, China

## Correspondence to

Professor Lin Shen;  
linshenpku@163.com

Dr Zhi Peng;  
zhipeng3@hotmail.com

## ABSTRACT

**Background** Epstein-Barr virus (EBV)-associated gastric cancer (GC) (EBVaGC) is a distinct molecular subtype of GC with a favorable prognosis. However, the exact effects and potential mechanisms of EBV infection on immune checkpoint blockade (ICB) efficacy in GC remain to be clarified. Additionally, EBV-encoded RNA (EBER) in situ hybridization (ISH), the traditional method to detect EBV, could cause false-positive/false-negative results and not allow for characterizing other molecular biomarkers recommended by standard treatment guidelines for GC. Herein, we sought to investigate the efficacy and potential biomarkers of ICB in EBVaGC identified by next-generation sequencing (NGS).

**Design** An NGS-based algorithm for detecting EBV was established and validated using two independent GC cohorts (124 in the training cohort and 76 in the validation cohort). The value of EBV infection for predicting ICB efficacy was evaluated among 95 patients with advanced or metastatic GC receiving ICB. The molecular predictive biomarkers for ICB efficacy were identified to improve the prediction accuracy of ICB efficacy in 22 patients with EBVaGC.

**Results** Compared with orthogonal assay (EBER-ISH) results, the NGS-based algorithm achieved high performance with a sensitivity of 95.7% (22/23) and a specificity of 100% (53/53). EBV status was identified as an independent predictive factor for overall survival and progression-free survival in patients with DNA mismatch repair proficient (pMMR) GC following ICB. Moreover, the patients with EBV+/pMMR and EBV-/MMR deficient (dMMR) had comparable and favorable survival following ICB. Twenty-two patients with EBV+/pMMR achieved an objective response rate of 54.5% (12/22) on immunotherapy. Patients with EBVaGC with a high cytotoxic T lymphocyte-associated antigen-4 (CTLA-4) level were less responsive to anti-programmed death-1/ligand 1 (PD-1/L1) monotherapy, and the combination of anti-CTLA-4 plus anti-PD-1/L1 checkpoint blockade benefited patients with EBVaGC more than anti-PD-1/L1 monotherapy with a trend close to significance ( $p=0.074$ ). There were nearly significant differences in tumor mutational burden (TMB) level and *SMARCA4* mutation frequency between the ICB response and non-response group.

**Conclusions** We developed an efficient NGS-based EBV detection strategy, and this strategy-identified EBV infection was as effective as dMMR in predicting ICB efficacy in GC. Additionally, we identified CTLA-4, TMB, and *SMARCA4* mutation as potential predictive biomarkers of ICB efficacy in EBVaGC, which might better inform ICB treatment for EBVaGC.

## BACKGROUND

Epstein-Barr virus (EBV)-associated gastric cancer (GC) (EBVaGC) accounts for approximately 5%–10% of GC worldwide and is well recognized as a distinct molecular subtype of GC.<sup>1–4</sup> Several lines of evidence suggested that patients with EBVaGC tended to have fewer lymph node metastases and a better prognosis.<sup>5–7</sup> Among cohorts of advanced EBVaGC, response rates following anti-programmed death-1 (anti-PD-1) monotherapy were reported to range from 25% to 100%, but all higher than that of unselected patients with advanced GC.<sup>8–11</sup> Although the exact impacts and potential mechanisms of EBV infection on GC immune checkpoint blockade (ICB) efficacy remain to be clarified, there has been a growing interest in EBV as an emerging biomarker to inform clinical management of GC, especially ICB treatment.

EBV-encoded RNA (EBER) in situ hybridization (ISH) has long been regarded as the gold standard for detecting EBV. However, apart from commonly false-negative EBER-ISH results caused by RNA degradation, false-positive results might be generated in the presence of background hybridization caused by poorly fixed tissues, non-specific staining, or cross-reactivity.<sup>12–13</sup> Moreover, EBER-ISH does not allow for simultaneous characterization of other clinically relevant biomarkers such as tumor mutational burden (TMB), microsatellite instability (MSI), *HER2* amplification, and *NTRK* fusion as recommended by the National Comprehensive Cancer Network (NCCN) Guidelines for GC.<sup>14</sup> The advent of next-generation sequencing (NGS) offers a viable solution by accommodating EBV detection and the gene profile in numerous other cancer-related markers in one single assay. However, it has been only employed to interrogate the EBV genome for research purposes.<sup>15–16</sup> The

development and validation of NGS-based EBV detection intended for clinical use have never been reported.

In this work, we aimed to develop an efficient NGS-based EBV detection strategy that allows for parallel characterization of other genomic features. More importantly, we assessed the ability of EBV status to predict the benefit from ICB treatment and explored the predictive molecular markers which may be incorporated into EBV status to improve the accuracy of ICB efficacy prediction.

## METHODS

### Samples and study design

The study design and consort patient flow diagram were illustrated in online supplemental figures 1 and 2. Gene selection, algorithm development, and EBV score cut-off training were performed using 24 EBVaGC and 100 EBV-negative GC (EBVnGC) tissue samples. Technical validation was conducted in a cohort of 23 EBVaGC and 53 EBVnGC tissue samples. The 124 and 76 samples mentioned above were obtained from the Beijing Cancer Hospital with a confirmed histological diagnosis of advanced GC and available EBER-ISH results.

The correlation between EBV score and viral copy number by quantitative PCR (qPCR) was assessed using 20 GC DNA samples with EBV score  $>0.00005$  (excluding EBV genes that could not be detected at all) retrieved from the 3DMed Biobank (3D Medicines).

The repeatability and reproducibility of the EBV detection method were evaluated using four EBVaGC and four EBVnGC tissue samples randomly selected from the technical validation cohort. Each sample was detected for two runs with each run in quadruplicate under the same operating conditions. The data of replicates in the intra-assay were counted for the repeatability test, while the data of the two batches in the inter-assay precision study were collected and compared for reproducibility analysis.

To determine the limit of detection (LOD), EBV-transformed B lymphoblasts, BL1954, BL1395, BL2009, and BL1143, were purchased from the American Type Culture Collection, and the control white blood cells were obtained from a healthy donor.<sup>17,18</sup> Briefly, genomic DNA samples derived from four EBV-positive cell lines were diluted into the genomic DNA isolated from the control white blood cells, targeting four titration points, 2.5%, 5%, 10%, and 20%. The titration series were examined at a total cell input of  $5 \times 10^6$  and four different sequencing depths: 100 $\times$ , 300 $\times$ , 500 $\times$ , and 1000 $\times$ .

To evaluate the predictive value of EBV status in ICB efficacy in patients with GC and further identify the molecular markers predictive of ICB efficacy in patients with EBVaGC, 95 patients with advanced or metastatic GC treated with ICB at Beijing Cancer Hospital from June 21, 2017, to October 22, 2021, were included. The exact ICB drugs for these patients were summarized in online supplemental table 1. Among 95 patients, 66 were DNA mismatch repair (MMR) proficient (pMMR), and 29 were MMR deficient (dMMR), where MMR status

was identified by immunohistochemistry (IHC). The patients with pMMR comprised 22 patients with EBV+/pMMR and 44 patients with EBV-/pMMR, wherein EBV status was obtained via our NGS-based method. The patients with dMMR were EBV negative and represented as EBV-/dMMR phenotype. All tumor samples had at least 20% tumor content as reviewed by two independent pathologists.

IHC, qPCR, NGS, EBER-ISH, and multiplex immunofluorescence (mIF) were described in online supplemental methods and online supplemental table 6.

### ICB efficacy evaluation

De-identified clinicopathological and efficacy data were extracted from patients' medical records by two independent physicians and were reviewed by a third physician in case of inconsistency. Tumor response was assessed as per the Response Evaluation Criteria in Solid Tumors, V.1.1, and categorized as complete response (CR), partial response (PR), stable disease (SD), and disease progression (PD). Objective response rate (ORR) was defined as CR plus PR. Progression-free survival (PFS) was defined as the time from the onset of ICB treatment to PD or death, whichever occurred first. Overall survival (OS) was defined as the time from the onset of ICB treatment to death as a result of any cause. The duration of response was defined as the interval from first documented CR or PR until PD or death by any cause, whichever occurred first. All samples were obtained with informed consents.

### Statistical analyses

Continuous variables were compared using a Student's t-test or the non-parametric Mann-Whitney U test, while categorical variables were compared using the  $\chi^2$  test or the Fisher's exact test where appropriate. Survival curves were plotted with the Kaplan-Meier method and analyzed using a log-rank test. Univariate and multivariate Cox regression analyses were applied to identify independent prognostic variables for ICB efficiency. Simple linear regression was adopted to examine the relationship between EBV copy number and EBV score. The receiver operating characteristic (ROC) analysis was performed using the web tool EasyROC (<http://www.biosoft.hacettepe.edu.tr/easyROC/>). All tests were two-sided, and a p value of  $<0.05$  was considered statistically significant. Statistical analyses were performed using R software V.3.6.1 (R Foundation for Statistical Computing), Python software V.3.9.5, GraphPad Prism V.7.01 (GraphPad Software), and SPSS V.22.0 (IBM).

## RESULTS

### Algorithm development for EBV detection

The study design was illustrated in online supplemental figure 1. To select target genes for EBV detection, *BHRF1* and *BCLF1* were excluded upfront for sharing significant homology with the human genome.<sup>19,20</sup> Regions with a high GC content were also excluded due to affecting library preparation/construction.<sup>21</sup> The rest of the

genome sequences were evaluated by their relevance to EBV pathogenesis and carcinogenesis, and six genes, *EBNA-1*, *EBNA-2*, *EBNA-3*, *LMP1*, *LMP2*, and *BZLF1*, were included in the EBV detection panel.<sup>22,23</sup> For each gene, a set of probes was designed to cover the whole exons. Since EBV viruses are classified into type 1 and type 2 based on *EBNA-2* and *EBNA-3* sequences, two sets of probes targeting type 1 and type 2 sequences separately were developed for each of the two genes.

Tissue samples from 24 patients with EBVaGC and 100 patients with EBVnGC as a training set were subjected to NGS analysis using a panel combining the EBV detection probes and the probes covering the whole exons of 733 cancer-related genes, including all currently available biomarkers related to tumor immunotherapy, targeted therapy, chemoradiotherapy, and prognosis (the gene list shown in online supplemental table 2). The sequencing depth was calculated for each EBV gene and multiplied by two before normalization using the sequencing depth of the 733-panel genes to obtain a normalized depth (NorDepth) for each gene. Due to low capture efficiency, *LMP1* and *LMP2* were excluded (online supplemental figure 3). The remaining four genes had a sharply higher NorDepth in the tumors from patients with EBVaGC than EBVnGC (figure 1A), which were included in the final panel. EBV score was defined as the median of the NorDepths of these four genes. In the training set, EBV score could significantly discriminate EBVaGC from EBVnGC ( $p < 0.001$ ) (figure 1B).

Additionally, 20 GC DNA samples were quantified for EBV load by qPCR. A strong correlation was observed between EBV score and EBV copy number ( $R^2 = 0.9326$ ,  $p < 0.001$ , figure 1C), corroborating the reliability of EBV score to reflect EBV status. The optimal cut-off EBV score for the definition of EBV positivity was determined at 0.05695 using the ROC curves, with an area under the curve (AUC) of 1. Furthermore, we found that the positive relation between EBV score and EBV copy number also held for the individual EBV gene, and the AUC values for EBV positivity predictions were 0.969 for *EBNA-1*, 0.865 for *EBNA-2*, 0.875 for *EBNA-3*, and 0.906 for *BZLF1* (online supplemental figure 4A,B). These results indicated that the EBV algorithm based on NGS detection of four EBV genes was established and could accurately identify EBVaGC.

### Technical validation

The accuracy of the EBV algorithm defining EBVaGC with an EBV score of at least 0.05695 was validated in a cohort of 76 advanced GC tumor samples, where 23 were diagnosed as EBVaGC and 53 as EBVnGC by EBER-ISH previously. Our NGS-based method identified 95.7% (22/23, 95% CI 77.3% to 99.8%) of EBVaGC tumors and 100% (53/53, 95% CI 93.2% to 100%) of the EBVnGC tumors, for an overall accuracy of 98.7% (75/76, 95% CI 92.9% to 99.9%) (figure 1D, online supplemental table 3). The positive predictive value was 100% (22/22, 95% CI 85.1% to 100%). The repeatability and reproducibility of the

EBV detection method were also assessed. Eight samples tested in two batches could get the same EBV status with 100% concordance (online supplemental table 4). The results of LOD showed that for all four EBV-positive cell lines, the EBV score of each sample was well above 0.05695 when the dilution was above 5% across different sequencing depths (figure 1E). Therefore, the LOD was determined as 5% at a sequencing depth of 100 $\times$ .

### EBV infection predicts clinical benefit from ICB

As existing evidence on the sensitivity of patients with EBVaGC to ICB remained controversial,<sup>8–10,24</sup> 95 patients with advanced or metastatic GC receiving ICB therapy were included to evaluate the predictive value of EBV infection in ICB efficacy. In 95 patients, 29 were dMMR, and 66 were pMMR consisting of 22 patients with EBV+/pMMR and 44 patients with EBV-/pMMR. EBV status in patients with pMMR was identified by our NGS-based method. Patients' baseline characteristics were summarized in table 1. In patients with pMMR, patients with EBV+/pMMR had a significantly higher proportion of responders than patients with EBV-/pMMR ( $p = 0.008$ ) (figure 2A). The survival analyses showed that patients with EBV+/pMMR had significantly favorable PFS (median PFS (mPFS) 8.5 vs 2.0 months,  $p < 0.001$ ) and OS (median OS (mOS) not reached (NR) vs 5.0 months,  $p = 0.002$ ) after ICB compared with patients with EBV-/pMMR (figure 2B,C). Univariate survival analyses revealed that ICB strategy, EBV status, prior systemic therapy, and age were significantly associated with PFS and OS (figure 2D, online supplemental table 5). Multivariate analysis indicated that EBV status remained a strong prognostic factor for PFS (HR 0.39, 95% CI 0.16 to 0.97,  $p = 0.042$ ) in patients with pMMR GC following ICB (figure 2E). Of note, there were two patients with EBV-negative by NGS and EBV-positive by EBER-ISH, both of whom were categorized into the EBV-/pMMR set. In the two patients, the PFS was 2.0 and 3.0 months, respectively, and OS was 3.2 and 10.4 months, respectively, which verged on the mPFS (2.0 months) and mOS (5.0 months) of the EBV-/pMMR group.

MSI-H/dMMR is a well-established biomarker for immunotherapy.<sup>14</sup> In the 22 patients with EBV+/pMMR, that is, EBVaGC, 12 achieved PR, five showed SD, and five experienced PD, yielding an ORR of 54.5% (95% CI 33.7% to 75.4%) (figure 2F), which was significantly higher than the ORR of 17.7% ( $p = 0.008$ ) in the EBV-/pMMR group and comparable to the EBV-/dMMR group ( $p = 0.768$ , online supplemental figure 5A,B) independent from the ICB strategy (data not shown). The median time to response was 1.8 months (range 1.1–5.6 months) in patients with EBVaGC (figure 2G). Besides, the ORR to ICB in patients with EBVaGC was less affected by prior lines of therapy ( $p = 0.378$ ) (online supplemental figure 6). The survival analyses showed that the patients with EBV+/pMMR and EBV-/dMMR had comparable and favorable PFS and OS, both of whom derived more survival benefit from ICB than the patients with EBV-/

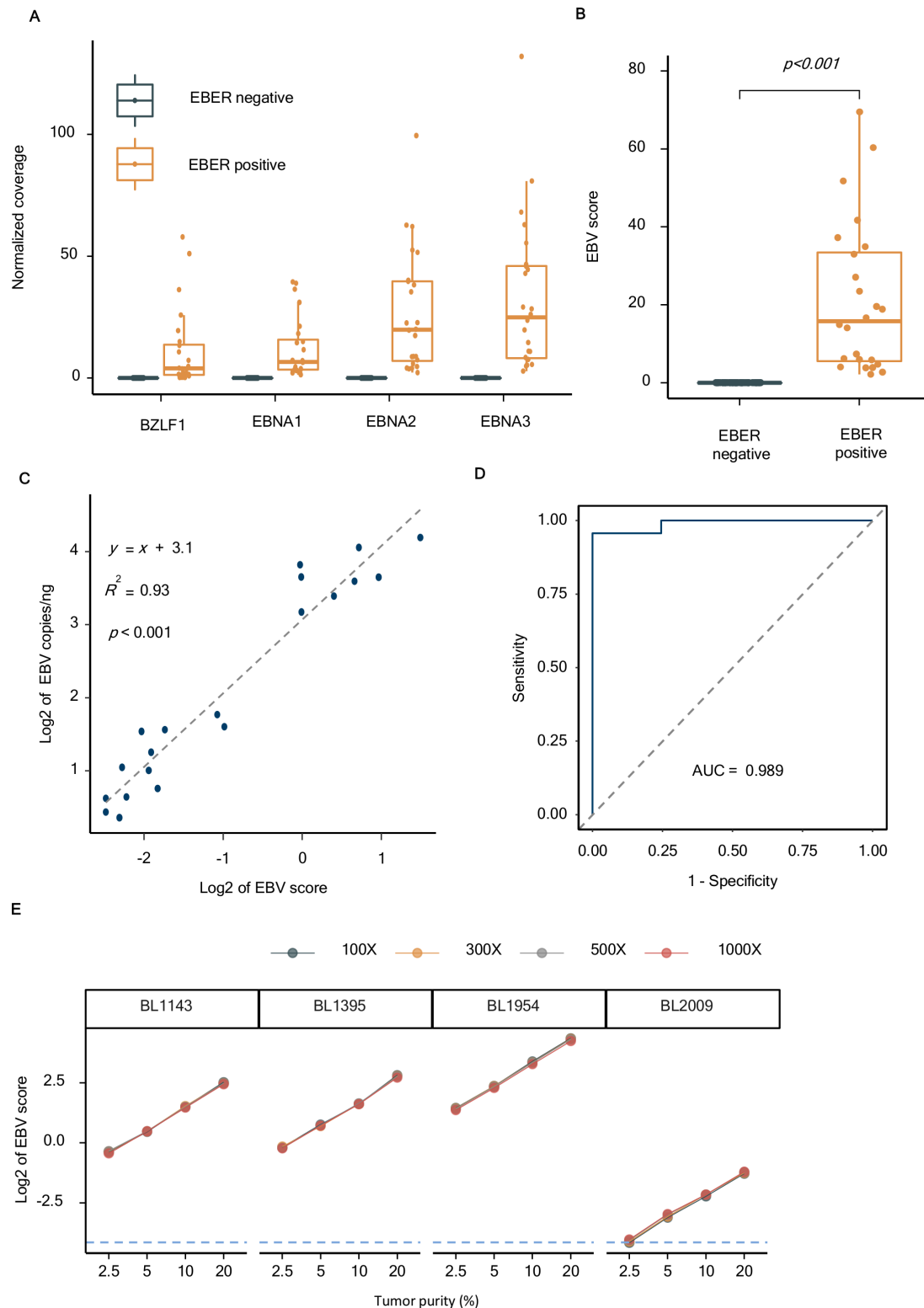


**Figure 1** Establishment and validation of NGS-based EBV detection method. (A,) Normalized coverage of EBV genes in 124 GC tissue samples which EBV status was identified by EBER-ISH. (B,) NGS algorithm-developed EBV score of 124 GC tissue samples with EBV status identified by EBER-ISH. (C,) The linear correlation between NGS algorithm-developed EBV score and the EBV copy number determined by TaqMan probe based absolute quantitative PCR of *BamHI* W fragment in 20 tumor tissue samples from patients with GC. (D,) the ROC curve of EBV score for predicting EBV status in 76 GC tissue samples where EBV status was previously identified by EBER-ISH. The area under the ROC curve was 0.989 (95% CI 0.968 to 1). (E,) Four EBV transformed cell lines were diluted to four concentrations (2.5%, 5%, 10%, and 20%) with blood white cells, and the normalized EBV score at each concentration under four sequencing depths (100×, 300×, 500× and 1000×) were detected and calculated. AUC, area under the curve; EBV, Epstein-Barr virus; EBER, Epstein-Barr virus-encoded small RNA; GC, gastric carcinoma; ISH, in situ hybridization; NGS, next-generation sequencing; ROC, receiver operator characteristic.

**Table 1** Baseline characteristics of the patients with gastric carcinoma received ICB therapy

Characteristics	EBV+/pMMR (n=22)	EBV-/pMMR (n=44)	EBV-/dMMR (n=29)	P value: EBV+/pMMR versus EBV-/pMMR	P value: EBV+/pMMR versus EBV-/dMMR
Age Median (range)	63.5 (28–74)	59.0 (24–77)	65.0 (32–82)	0.320	0.266
EBV status by EBER					
Positive	22	2	0	0.000	0.000
Negative	0	36	23		
Sex					
Male	18	31	19	0.384	0.225
Female	4	13	10		
Stage					
III	1	0	4	0.333	0.375
IV	21	44	25		
Prior systemic therapy					
Yes	13	43	23	0.000	0.135
No	9	1	6		
ICB strategy					
Mono-ICB	8	43	25	0.000	0.000
Dual-ICB	14	1	4		
PD-L1 (CPS >1)					
Positive	15	19	13	0.115	1.000
Negative	7	23	7		
HER2 IHC staining					
0	16	26	18	0.088	0.906
1	4	3	7		
2	1	13	2		
3	1	2	1		

CPS, combined positive score; dMMR, mismatch repair deficient; Dual-ICB, combination anti-CTLA-4 plus anti-PD-1/L1 therapy; EBER, Epstein-Barr virus-encoded small RNA; EBV, Epstein-Barr virus; HER2, human epidermal growth factor receptor 2; ICB, immune checkpoint blockade; ICI, immune checkpoint inhibitor; IHC, immunohistochemistry; Mono-ICB, anti-PD-1/L1 monotherapy; PD-1, programmed death 1; PD-L1, programmed death-ligand 1; pMMR, mismatch repair proficient.

pMMR (online supplemental figure 5C,D). A multivariable Cox regression analysis also confirmed that EBV and dMMR had equal effectiveness in predicting PFS regardless of monotherapy or combination therapy (online supplemental figure 5E).

#### Identification of the predictive factors for ICB efficacy in patients with EBVaGC

Based on published literature highlighting the role of EBV infection in promoting an inflamed tumor immune microenvironment (TME),<sup>25</sup> the density of multiple lymphocyte subgroups and the proposed ICB biomarker-expressed cells were determined in 22 EBVaGC. Three EBVaGC with no available tissues and two EBVaGC with poor-quality tissue samples were excluded from this analysis. The mIF assay revealed that only the density of cytotoxic T lymphocyte-associated antigen-4 (CTLA-4)<sup>+</sup> and T cell immunoglobulin-3 (TIM-3)<sup>+</sup> cells in the tumor was significantly higher in the ICB non-response group than in the response group, while no significant difference

was observed in other cell subgroups between the ICB response and non-response group (figure 3A, online supplemental figure 7). The representative images of mIF staining were displayed in online supplemental figure 8. In eight patients receiving programmed death-1/ligand 1 (PD-1/L1) monotherapy, CTLA-4 expression level in six patients who did not reach response was numerically higher than that in two patients with PR (data not shown). Additionally, in 14 patients receiving the combination of CTLA-4 and PD-1/L1 blockers, 10 reached PR, two showed SD, and two experienced PD. The patients receiving dual-ICB therapy had a better response than those who administered mono-immunotherapy with a tendency toward statistical significance (p=0.074) (figure 3B). Accordingly, the dual-ICB-treated patients tended to have a better PFS than the patients undergoing mono-immunotherapy (online supplemental figure 9). Consistent results were observed in another three patients with EBVaGC with ICB as neoadjuvant therapy.

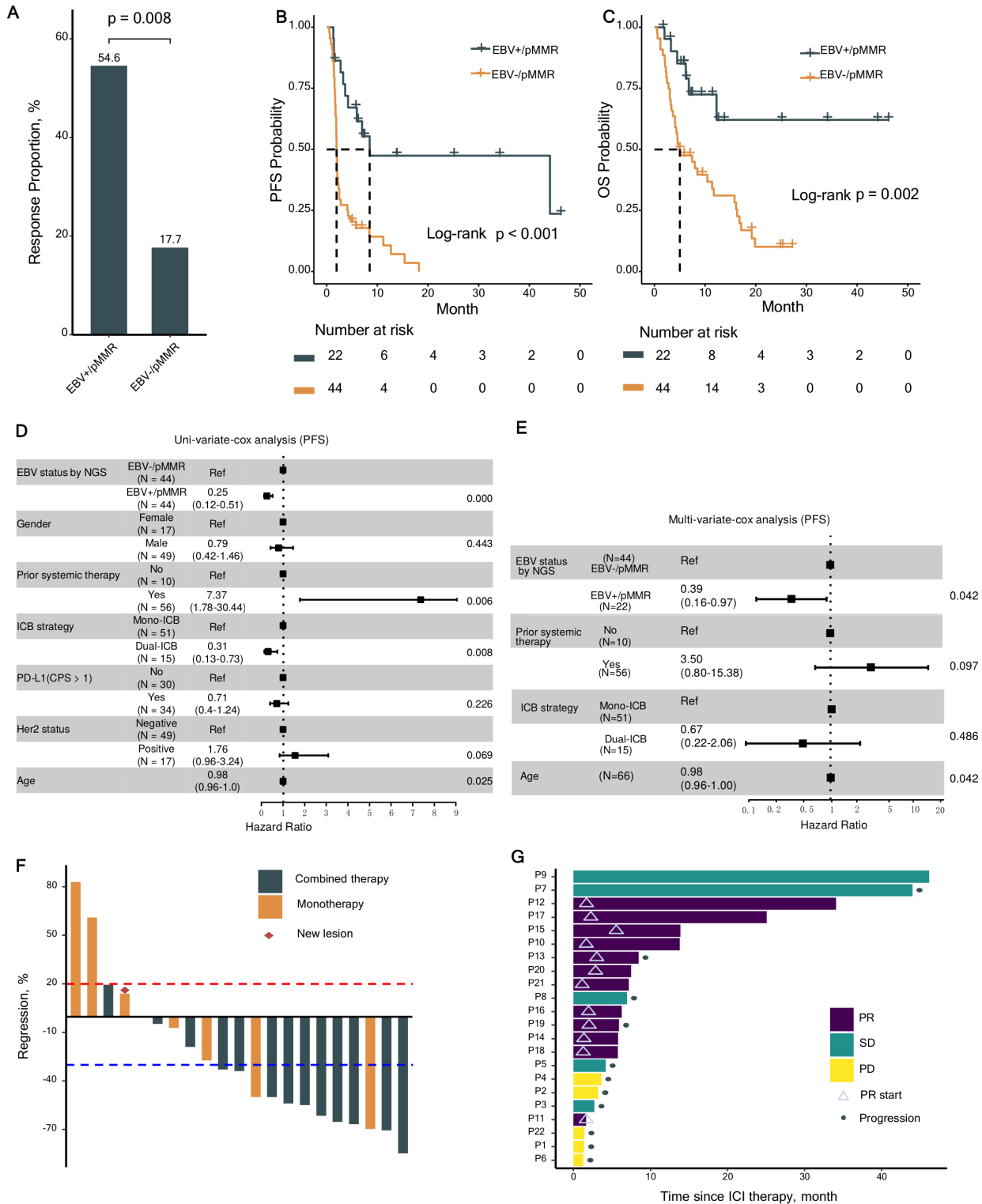


**Figure 2** EBV infection as a predictive biomarker for patients with GC receiving ICB. A, the percentage of responders and non-responders in patients with EBV-/pMMR and EBV+/pMMR. Kaplan-Meier curve of PFS (B) and OS (C) in patients with pMMR receiving immunotherapy where EBV status was determined by NGS. Univariate (D) and multivariate (E) analysis of the variables associated with PFS of patients with pMMR treated with immunotherapy. Tumor regression from baseline (F) and time to response and duration of response (G) in 22 patients with EBVaGC receiving immunotherapy. CPS, combined positive score; CTLA-4, cytotoxic T lymphocyte-associated antigen-4; Dual-ICB, combination anti-CTLA-4 plus anti-PD-1/L1 therapy; EBV, Epstein-Barr virus; EBVaGC: Epstein-Barr virus-associated gastric carcinoma; GC, gastric cancer; ICB, immune checkpoint blockade; ICI, immune checkpoint inhibitor; Mono-ICB, anti-PD-1/L1 monotherapy; NGS, next-generation sequencing; PD, progressive disease; PD-1/L1, programmed death-1/ligand 1; PFS, progression-free survival; pMMR, mismatch repair proficient; PR, partial response; SD, stable disease.

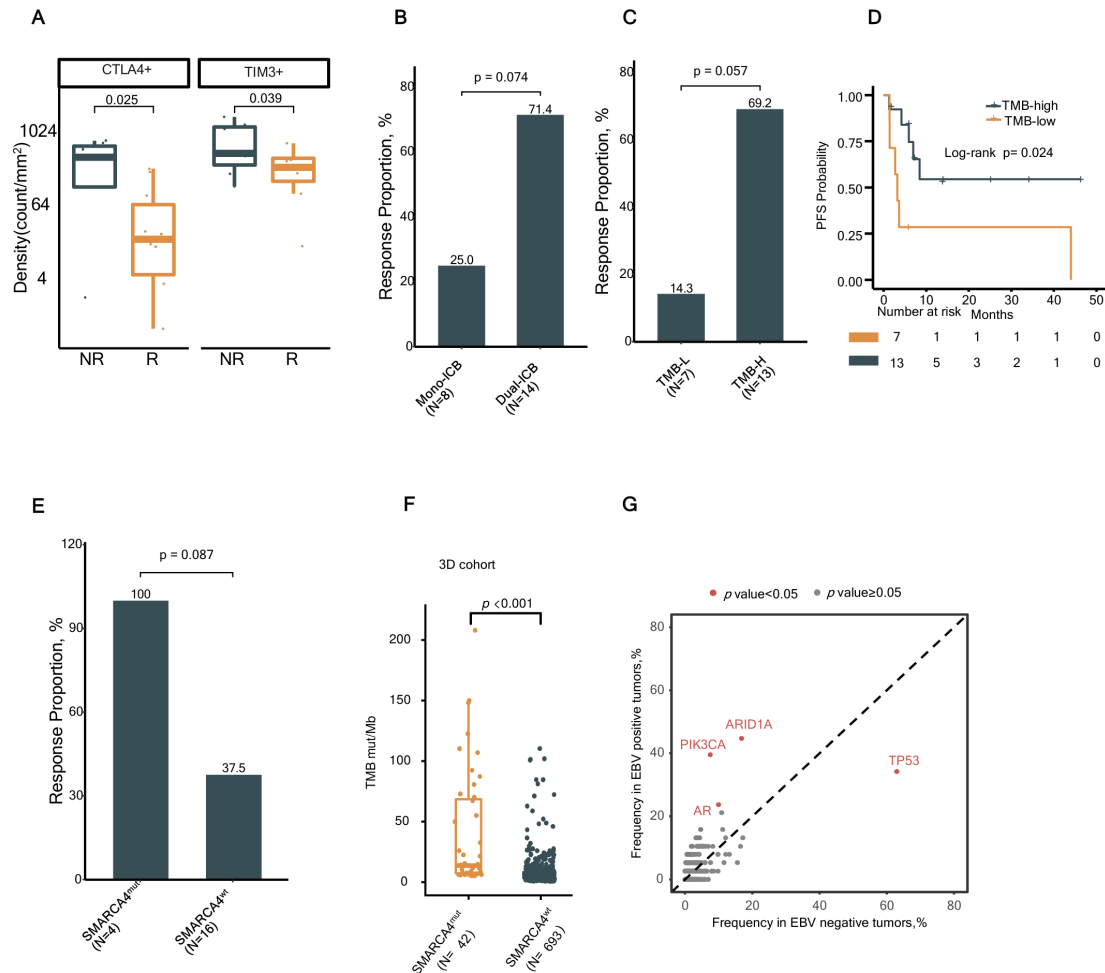


**Figure 3** Biomarkers for patients with EBVaGC receiving ICB. Twenty-two patients with EBVaGC consisting of 12 ICB responders and 10 non-responders were analyzed to identify potential predictive biomarkers of ICB efficacy. (A), The density of CTLA-4<sup>+</sup> and TIM3<sup>+</sup> cells in tumor region from responders and non-responders. (B,) The percentage of responders and non-responders after administration of mono-immunotherapy or dual-immunotherapy. (C,) The percentage of responders and non-responders in TMB-low and TMB-high patients. (D,) Kaplan-Meier curve of PFS between TMB-low and TMB-high patients. (E,) The percentage of responders and non-responders in the patients with or without *SMARCA4* mutation. (F), The TMB level in 735 GC cohort tumor tissues with or without *SMARCA4* mutation from the 3DMed Biobank. (G,) The frequency variation of gene mutations between patients with EBVaGC and EBVnGC in 735 GC cohort from 3DMed Biobank using a 733-gene panel. CTLA-4, cytotoxic T lymphocyte-associated antigen-4; Dual-ICB, combination anti-CTLA-4 plus anti-PD-1/L1 therapy; EBV, Epstein-Barr virus; EBVaGC, EBV-associated gastric cancer; EBVnGC, EBV-negative gastric cancer; ICB, immune checkpoint blockade; Mono-ICB, mono-immunotherapy; mut, mutation; NR, non-responder; PD-1/L1, programmed death-1/ligand 1; PFS, progression-free survival; R, Responder; *SMARCA4*, SWI/SNF related, matrix associated, actin dependent regulator of chromatin, subfamily A, member 4; Tim-3, T cell immunoglobulin-3; TMB, tumor mutation burden; TMB-H, high TMB; TMB-L, low TMB; WT, wild type.

The one with anti-PD-1 monotherapy did not reach clinical benefit, while two dual-ICB treated patients separately achieved pathological PR and pathological CR.

Since TMB also impacts the efficacy of immunotherapy in GC and its test has been recommended by the NCCN Guidelines, we also analyzed TMB level by NGS in 22 patients with EBVaGC, excluding two EBVaGC with poor-quality tissue samples. TMB level was higher in the ICB response group than in the non-response group but failed to achieve a customary level of statistical significance ( $p=0.140$ ) (data not shown). When 20 patients with EBVaGC were classified as TMB-high or TMB-low using the top quartile threshold (8.82 per Mb) generated from

47 patients with EBVaGC with 24 in the training and 23 in the validation cohort, TMB-high patients had a significantly longer PFS (mPFS NR vs 3.2 months,  $p=0.024$ ) along with a trend toward better response (ORR 69.2% vs 14.3%,  $p=0.057$ ) than TMB-low patients (figure 3C,D).

Next, the gene mutations were investigated. The frequently mutated genes were listed in online supplemental figure 10. *SMARCA4* gene mutation occurred more commonly in the response group than the non-response group with a borderline level of statistical significance (40% vs 0%,  $p=0.087$ ). All the patients with *SMARCA4* mutation attained a PR following ICB and had a numerically higher PFS than wild-type *SMARCA4*

patients (figure 3E, online supplemental figure 11). Additionally, the frequency of *SMARCA4* mutation was analyzed and exhibited no significant difference between EBVaGC and EBVnGC in a 735 Chinese patients with GC cohort retrieved from the 3DMed Biobank (data not shown). These data suggested that *SMARCA4* mutation might be a promising predictor of ICB efficacy in patients with EBVaGC.

Considering that patients with *SMARCA4* mutation are reported to benefit more from ICB in non-small cell lung cancer via increasing TMB,<sup>26</sup> the effects of *SMARCA4* mutation on TMB were also analyzed. The patients with *SMARCA4* alteration possessed a higher TMB level than patients with wild-type *SMARCA4*, which reached borderline significance in 20 patients with EBVaGC ( $p=0.098$ ) and statistical significance in the Chinese GC cohort ( $p<0.001$ ) (figure 3F).

Characterization of EBVaGC was performed via a 735-case Chinese GC cohort using our EBV algorithm along with the 733-gene panel. About 5.2% (38/735) of the patients were identified as EBVaGC. The mutational profiles showed that mutations in *ARID1A* (44.7% (17/38),  $p<0.001$ ), *PIK3CA* (39.5% (15/38),  $p<0.001$ ), and *AR* (23.7% (9/38),  $p=0.029$ ) were recurrent in EBVaGC, while alterations in *TP53* (63.0% (439/697),  $p<0.001$ ) were enriched in EBVnGC (figure 3G).

## DISCUSSION

Herein we innovatively developed an NGS-based EBV detection strategy which allows for simultaneous characterization of other genomic features of patients with GC. Our EBV algorithm demonstrated a sensitivity of 95.7%, a specificity of 100%, and an overall accuracy of 98.7% in reference to EBER-ISH in the validation cohort. Moreover, EBV infection predicted response in 54.5% of an ICB-treated cohort, which was as effective as dMMR in predicting favorable outcomes for patients with ICB-treated GC. TME analysis revealed that patients with EBVaGC with high CTLA-4 levels were less responsive to single-agent anti-PD-1/L1 therapy, and EBVaGC derived greater benefit from combination PD-1/L1 plus CTLA-4 blockade than anti-PD-1/L1 monotherapy. Further investigation identified that TMB and *SMARCA4* mutation might be predictive biomarkers of ICB efficacy in patients with EBVaGC.

Ever since EBVaGC was recognized as a distinct molecular subtype, EBV has gained widespread attention as a potential biomarker to guide the personalized management of GC.<sup>2 27</sup> Given the considerable heterogeneity of GC and the challenge with tissue availability, it is highly desirable to profile other biomarkers along with EBV in one single assay.<sup>28 29</sup> However, most previously reported NGS-based EBV detection involved sequencing of the entire EBV genome, and none of them incorporated EBV with cancer-related genes in the same panel, rendering them less practical for clinical use.<sup>15 16</sup> In our EBV detection panel, the four EBV genes were analyzed with the

cancer-related genes together, and therefore this method may be more cost-effective and feasible to be applied in clinical practice. Additionally, both algorithm development and validation were performed using clinical samples, ensuring the overall accuracy and reliability of the algorithm.

Advanced GC has a dismal prognosis with a 5-year survival rate of  $<30\%$  and a limited number of effective therapeutic options.<sup>30</sup> Despite the approval of ICB for treating chemorefractory GC, response to monotherapy was reported in only 11.2%–12% of unselected patients.<sup>24 31 32</sup> Although Food and Drug Administration approved pembrolizumab for patients with PD-L1 positive chemorefractory GC, a combined positive score of  $\geq 1$  was only associated with an ORR of 15.5%–22%.<sup>32 33</sup> dMMR/MSI-H represents an effective marker by predicting an ORR of 45.8%–85.7% among metastatic patients.<sup>24 32 34</sup>

However, around 80% of patients with GC are classified as pMMR. EBVaGC is a particular subtype of GC, and EBV infection is considered to be a potential biomarker for the response to immunotherapy in GC.<sup>1 2 8–10 24</sup> In our cohort of 22 patients with advanced EBVaGC, a 54.5% ORR and an mPFS lasting 8.47 months were achieved following ICB, which were significantly improved compared with the unselected patients with GC treated with mono-immunotherapy (11.2% ORR and mPFS 1.61 months) and dual-ICB therapy (24% ORR and mPFS 1.4 months).<sup>24 31 32</sup> Further analysis showed that EBV status was comparably effective as dMMR/MSI-H as an independent predictive factor for ICB efficacy in GC. Notably, two patients with EBV negativity by NGS but positivity by EBER-ISH had poor and comparable survival with patients with EBV-/pMMR. One had similar molecular characteristics with patients with EBVnGC, such as TP53 mutation (c.844C>T), while the other had a deleterious *BCOR* mutation, which might account for the poor benefit from ICB for that *BCOR* deletion had been documented to perturb dendritic cell development.<sup>35</sup> These phenomena might be reminiscent of the EBV status detected by NGS with high accuracy of ICB efficacy prediction and potential false positivity of EBV identification by EBER-ISH. Given the challenge of false-positive/false-negative EBER-ISH results, incorporating NGS-based methods may improve the diagnostic accuracy of EBV-related diseases and better inform follow-up treatment.

EBV infection has been reported to increase tumor-infiltrating lymphocytes and the expression of immune checkpoint molecules, thereby invoking clinical response to ICB.<sup>36 37</sup> We further investigated the TME difference between the ICB responders and non-responders in EBVaGC and found that the density of CTLA-4<sup>+</sup> cells and TIM-3<sup>+</sup> cells was significantly higher in the non-response group than in the response group. High CTLA-4 expression on helper T cells causes the immunosuppressive microenvironment.<sup>38</sup> As expected, patients with EBVaGC with high CTLA-4 levels were less responsive to anti-PD-1/L1 monotherapy, and EBVaGC derived more benefit from combination PD-1/L1 plus CTLA-4 blockade than



anti-PD-1/L1 monotherapy. TIM-3, standing for T-cell immunoglobulin and mucin domain 3, is a crucial immune checkpoint and negatively affects the immune system via complex biology.<sup>39,40</sup> One recent study showed that the TIM-3<sup>+</sup> cell infiltration was associated with an immunoevasive GC subtype with CD8<sup>+</sup> T cell dysfunction and identified that TIM-3 might serve as a promising target for immunotherapy in GC.<sup>41</sup> Another recent study reported that combining anti-PD-1 and anti-TIM-3 mAb had an additive effect on the cytotoxicity of cytotoxic T lymphocytes, suggesting the dual-ICB targeting for PD-1 and TIM-3 as a means of increasing response rates in GC.<sup>42</sup> Based on these findings, triple blockade therapy targeting PD-1, CTLA-4, and TIM-3 might be a rational approach to benefit the patients with EBVaGC with the high density of CTLA-4<sup>+</sup> and TIM-3<sup>+</sup> cells.

Extensive analyses about genomic features were also conducted comparing ICB responders and non-responders to find possible pretreatment biomarkers predictive of response or resistance. *SMARCA4* is the most commonly mutated member of the chromatin remodeling SWI/SNF complex. Some evidence suggested that improved activity of ICB in *SMARCA4*-deficient cancers might be owing to the increased TMB and activated TME.<sup>26,43,44</sup> Consistently, our findings from 22 EBVaGC and 735-case Chinese GC cohort showed that *SMARCA4* mutation might be a positive predictor of ICB efficacy in EBVaGC, and the patients with *SMARCA4* mutation attained PR, which might be owing to the increased TMB.

It has been documented that EBV-associated tumors have distinct molecular and TME characteristics, which may guide more targeted clinical treatment.<sup>45–47</sup> Combining the EBV algorithm with the 733-gene panel, we identified EBV prevalence in a Chinese cohort of 735 patients with GC as well as the landscape of their molecular characteristics. EBVaGC accounted for 5.2% of the cohort, almost identical with the prevalence of 5.1% for EBV previously reported among Chinese patients with GC.<sup>3</sup> Consistent with previous studies,<sup>45,48–50</sup> EBVaGC tumors were characterized with a high prevalence of *ARID1A*, *PIK3CA*, and *AR* mutations, all of which were associated with improved antitumor immunity or sensitivity to ICB in solid tumors, while EBVnGC had a higher frequency of mutations in TP53, whose mutations had been reported associated with poorer ICB efficacy in patients with pMMR GC, supporting that patients with EBVaGC had a greater likelihood of benefit from ICB than patients with EBVnGC.<sup>51–54</sup>

The relatively small sample size of the EBVaGC ICB-treatment cohort, although it was the largest to date, represents the main limitation of our study. This study included predictive biomarker analysis about ICB efficacy and identified that CTLA-4, TMB, and *SMARCA4* mutation might be predictive biomarkers of ICB efficacy in EBVaGC. Due to the small sample sizes and ethnically homogeneous populations for these analyses, these results are challenging, and caution should be applied in extrapolating these results to patients of other ethnicities.

Prospective trials with larger sample sizes and different ethnic populations are warranted to confirm these findings.

In summary, our NGS-based EBV detection method is accurate and reliable and enables comprehensive molecular diagnosis of EBVaGC with specific implications for ICB efficacy prediction.

**Acknowledgements** We thank the staff Bei Zhang, Hui Chen, Shiqing Chen, Hao Chen, Jie Wang, Yunjie Song, Lei Wang, and Youbing Guo of the 3D Medicines for their valuable contributions in statistical analysis and critical revision of the manuscript for important intellectual content.

**Contributors** LS is responsible for the overall content as the guarantor. LS accepts full responsibility for the work and/or the conduct of the study, had access to the data, and controlled the decision to publish. LS and ZP conceived and designed this study and reviewed and corrected the manuscript. YB, TX, ZW, ST, XZ, FZ, and XW were involved in the data collection and interpretation. JC, ST, and XZ drafted the manuscript. FZ performed the statistical analysis. YB and TX revised the manuscript.

**Funding** This study was supported by the Fundamental Research Funds for the Central Universities/Peking University Clinical Medicine Plus X-Young Scholars Project (No. PKU2021LCXQ016), the third round of public welfare development and reform pilot projects of Beijing Municipal Medical Research Institutes (Beijing Medical Research Institute, 2019-1), and the Key Program of Beijing Natural Science Foundation (No. Z210015).

**Competing interests** ST, FZ, XZ, and JC are employees of 3D Medicines.

**Patient consent for publication** Not applicable.

**Ethics approval** The study was approved by the institutional review board of Beijing Cancer Hospital (Approval ID: 2019YJZ56). Participants gave informed consent to participate in the study before taking part.

**Provenance and peer review** Not commissioned; externally peer reviewed.

**Data availability statement** All data relevant to the study are included in the article or uploaded as supplementary information.

**Supplemental material** This content has been supplied by the author(s). It has not been vetted by BMJ Publishing Group Limited (BMJ) and may not have been peer-reviewed. Any opinions or recommendations discussed are solely those of the author(s) and are not endorsed by BMJ. BMJ disclaims all liability and responsibility arising from any reliance placed on the content. Where the content includes any translated material, BMJ does not warrant the accuracy and reliability of the translations (including but not limited to local regulations, clinical guidelines, terminology, drug names and drug dosages), and is not responsible for any error and/or omissions arising from translation and adaptation or otherwise.

**Open access** This is an open access article distributed in accordance with the Creative Commons Attribution Non Commercial (CC BY-NC 4.0) license, which permits others to distribute, remix, adapt, build upon this work non-commercially, and license their derivative works on different terms, provided the original work is properly cited, appropriate credit is given, any changes made indicated, and the use is non-commercial. See <http://creativecommons.org/licenses/by-nc/4.0/>.

#### ORCID iD

Lin Shen <http://orcid.org/0000-0003-1134-2922>

#### REFERENCES

- Lee J-H, Kim S-H, Han S-H, *et al.* Clinicopathological and molecular characteristics of Epstein-Barr virus-associated gastric carcinoma: a meta-analysis. *J Gastroenterol Hepatol* 2009;24:354–65.
- Cancer Genome Atlas Research Network. Comprehensive molecular characterization of gastric adenocarcinoma. *Nature* 2014;513:202–9.
- Qiu M-Z, He C-Y, Lu S-X, *et al.* Prospective observation: clinical utility of plasma Epstein-Barr virus DNA load in ebv-associated gastric carcinoma patients. *Int J Cancer* 2020;146:272–80.
- Chang MS, Kim DH, Roh JK, *et al.* Epstein-Barr virus-encoded BART1 promotes proliferation of gastric carcinoma cells through regulation of NF- $\kappa$ B. *J Virol* 2013;87:10515–23.
- van Beek J, zur Hausen A, Snel SN, *et al.* Morphological evidence of an activated cytotoxic T-cell infiltrate in EBV-positive gastric

- carcinoma preventing lymph node metastases. *Am J Surg Pathol* 2006;30:59–65.
- 6 Song H-J, Srivastava A, Lee J, et al. Host inflammatory response predicts survival of patients with Epstein-Barr virus-associated gastric carcinoma. *Gastroenterology* 2010;139:e82:84–92.
  - 7 Liu X, Liu J, Qiu H, et al. Prognostic significance of Epstein-Barr virus infection in gastric cancer: a meta-analysis. *BMC Cancer* 2015;15:782.
  - 8 Qiu M-Z, He C-Y, Yang D-J, et al. Observational cohort study of clinical outcome in Epstein-Barr virus associated gastric cancer patients. *Ther Adv Med Oncol* 2020;12:1758835920937434.
  - 9 Kubota Y, Kawazoe A, Sasaki A, et al. The impact of molecular subtype on efficacy of chemotherapy and checkpoint inhibition in advanced gastric cancer. *Clin Cancer Res* 2020;26:3784–90.
  - 10 Wang F, Wei XL, Wang FH, et al. Safety, efficacy and tumor mutational burden as a biomarker of overall survival benefit in chemo-refractory gastric cancer treated with toripalimab, a PD-1 antibody in phase Ib/II clinical trial NCT02915432. *Ann Oncol* 2019;30:1479–86.
  - 11 Kim ST, Cristescu R, Bass AJ, et al. Comprehensive molecular characterization of clinical responses to PD-1 inhibition in metastatic gastric cancer. *Nat Med* 2018;24:1449–58.
  - 12 Camargo MC, Bowlby R, Chu A, et al. Validation and calibration of next-generation sequencing to identify Epstein-Barr virus-positive gastric cancer in the cancer genome atlas. *Gastric Cancer* 2016;19:676–81.
  - 13 Gulley ML. Molecular diagnosis of Epstein-Barr virus-related diseases. *J Mol Diagn* 2001;3:1–10.
  - 14 (NCCN) NCCN. NCCN clinical practice Guideline in oncology. *Gastric Cancer* 2021.
  - 15 Liu P, Fang X, Feng Z, et al. Direct sequencing and characterization of a clinical isolate of Epstein-Barr virus from nasopharyngeal carcinoma tissue by using next-generation sequencing technology. *J Virol* 2011;85:11291–9.
  - 16 Chen J-N, Zhou L, Qiu X-M, et al. Determination and genome-wide analysis of Epstein-Barr virus (EBV) sequences in ebv-associated gastric carcinoma from Guangdong, an endemic area of nasopharyngeal carcinoma. *J Med Microbiol* 2018;67:1614–27.
  - 17 Gazdar AF, Kurvari V, Virmani A, et al. Characterization of paired tumor and non-tumor cell lines established from patients with breast cancer. *Int J Cancer* 1998;78:766–74.
  - 18 Caputo JL. Biosafety procedures in cell culture. *Journal of Tissue Culture Methods* 1988;11:223–7.
  - 19 Huang Q, Petros AM, Virgin HW, et al. Solution structure of the BHRF1 protein from Epstein-Barr virus, a homolog of human Bcl-2. *J Mol Biol* 2003;332:1123–30.
  - 20 Lindquester GJ, Greer KA, Stewart JP, et al. Epstein-Barr virus IL-10 gene expression by a recombinant murine gammaherpesvirus in vivo enhances acute pathogenicity but does not affect latency or reactivation. *Herpesviridae* 2014;5:1.
  - 21 Berenstein AJ, Lorenzetti MA, Preciado MV. Recombination rates along the entire Epstein Barr virus genome display a highly heterogeneous landscape. *Infect Genet Evol* 2018;65:96–103.
  - 22 Farrell PJ. Epstein-Barr virus and cancer. *Annu Rev Pathol* 2019;14:29–53.
  - 23 El-Sharkawy A, Al Zaidan L, Malki A. Epstein-Barr virus-associated malignancies: roles of viral oncoproteins in carcinogenesis. *Front Oncol* 2018;8:265.
  - 24 Janjigian YY, Bendell J, Calvo E, et al. CheckMate-032 study: efficacy and safety of nivolumab and nivolumab plus ipilimumab in patients with metastatic esophagogastric cancer. *J Clin Oncol* 2018;36:2836–44.
  - 25 Gullo I, Oliveira P, Athellogou M, et al. New insights into the inflamed tumor immune microenvironment of gastric cancer with lymphoid stroma: from morphology and digital analysis to gene expression. *Gastric Cancer* 2019;22:77–90.
  - 26 Schoenfeld AJ, Bandlamudi C, Lavery JA, et al. The Genomic Landscape of SMARCA4 Alterations and Associations with Outcomes in Patients with Lung Cancer. *Clin Cancer Res* 2020;26:5701–8.
  - 27 Röcken C. Molecular classification of gastric cancer. *Expert Rev Mol Diagn* 2017;17:293–301.
  - 28 Robert ME, Lamps L, Lauwers GY, et al. Recommendations for the reporting of gastric carcinoma. *Hum Pathol* 2008;39:9.e1–9.e12.
  - 29 Matsuoka T, Yashiro M. Biomarkers of gastric cancer: current topics and future perspective. *World J Gastroenterol* 2018;24:2818–32.
  - 30 Chen W, Zheng R, Baade PD, et al. Cancer statistics in China, 2015. *CA Cancer J Clin* 2016;66:115–32.
  - 31 Kang Y-K, Boku N, Satoh T, et al. Nivolumab in patients with advanced gastric or gastro-oesophageal junction cancer refractory to, or intolerant of, at least two previous chemotherapy regimens (ONO-4538-12, ATTRACTION-2): a randomised, double-blind, placebo-controlled, phase 3 trial. *Lancet* 2017;390:2461–71.
  - 32 Fuchs CS, Doi T, Jang RW, et al. Safety and efficacy of pembrolizumab monotherapy in patients with previously treated advanced gastric and gastroesophageal junction cancer: phase 2 clinical KEYNOTE-059 trial. *JAMA Oncol* 2018;4:e180013.
  - 33 Muro K, Chung HC, Shankaran V, et al. Pembrolizumab for patients with PD-L1-positive advanced gastric cancer (KEYNOTE-012): a multicentre, open-label, phase 1B trial. *Lancet Oncol* 2016;17:717–26.
  - 34 Marabelle A, Le DT, Ascierto PA, et al. Efficacy of pembrolizumab in patients with Noncolorectal high microsatellite Instability/Mismatch repair-deficient cancer: results from the phase II KEYNOTE-158 study. *J Clin Oncol* 2020;38:1–10.
  - 35 Tian L, Tomei S, Schreuder J, et al. Clonal multi-omics reveals BCOR as a negative regulator of emergency dendritic cell development. *Immunity* 2021;54:1338–51.
  - 36 Derks S, de Klerk LK, Xu X, et al. Characterizing diversity in the tumor-immune microenvironment of distinct subclasses of gastroesophageal adenocarcinomas. *Ann Oncol* 2020;31:1011–20.
  - 37 Panda A, Mehnert JM, Hirshfield KM, et al. Immune activation and benefit from Avelumab in EBV-positive gastric cancer. *J Natl Cancer Inst* 2018;110:316–20.
  - 38 Leach DR, Krummel MF, Allison JP. Enhancement of antitumor immunity by CTLA-4 blockade. *Science* 1996;271:1734–6.
  - 39 Solinas C, De Silva P, Bron D. Significance of Tim3 expression in cancer: from biology to the clinic. *Paper presented at: Seminars in oncology*, 2019.
  - 40 Friedlaender A, Addeo A, Banna G. New emerging targets in cancer immunotherapy: the role of Tim3. *ESMO Open* 2019;4:e000497.
  - 41 Chen K, Gu Y, Cao Y, et al. TIM3<sup>+</sup> cells in gastric cancer: clinical correlates and association with immune context. *Br J Cancer* 2022;126:1–9.
  - 42 Mimura K, Kua L-F, Xiao J-F, et al. Combined inhibition of PD-1/PD-L1, Lag-3, and Tim-3 axes augments antitumor immunity in gastric cancer-T cell coculture models. *Gastric Cancer* 2021;24:611–23.
  - 43 Takada K, Sugita S, Murase K, et al. Exceptionally rapid response to pembrolizumab in a SMARCA4-deficient thoracic sarcoma overexpressing PD-L1: a case report. *Thorac Cancer* 2019;10:2312–5.
  - 44 Henon C, Blay J-Y, Massard C, et al. Long lasting major response to pembrolizumab in a thoracic malignant rhabdoid-like SMARCA4-deficient tumor. *Ann Oncol* 2019;30:1401–3.
  - 45 Hong S, Liu D, Luo S, et al. The genomic landscape of Epstein-Barr virus-associated pulmonary Lymphoepithelioma-like carcinoma. *Nat Commun* 2019;10:3108.
  - 46 Huang Y-H, Zhang CZ-Y, Huang Q-S, et al. Clinicopathologic features, tumor immune microenvironment and genomic landscape of Epstein-Barr virus-associated intrahepatic cholangiocarcinoma. *J Hepatol* 2021;74:838–49.
  - 47 Derks S, Liao X, Chiaravalli AM, et al. Abundant PD-L1 expression in Epstein-Barr virus-infected gastric cancers. *Oncotarget* 2016;7:32925–32.
  - 48 Wang K, Kan J, Yuen ST, et al. Exome sequencing identifies frequent mutation of ARID1A in molecular subtypes of gastric cancer. *Nat Genet* 2011;43:1219–23.
  - 49 Böger C, Krüger S, Behrens HM, et al. Epstein-Barr virus-associated gastric cancer reveals intratumoral heterogeneity of PIK3CA mutations. *Ann Oncol* 2017;28:1005–14.
  - 50 Zheng X, Wang J, Wei L, et al. Epstein-Barr virus microRNA miR-BART5-3p inhibits p53 expression. *J Virol* 2018;92. doi:10.1128/JVI.01022-18. [Epub ahead of print: 01 12 2018].
  - 51 Borcoman E, De La Rochere P, Richer W, et al. Inhibition of PI3K pathway increases immune infiltrate in muscle-invasive bladder cancer. *Oncimmunology* 2019;8:e1581556.
  - 52 Hu G, Tu W, Yang L, et al. ARID1A deficiency and immune checkpoint blockade therapy: from mechanisms to clinical application. *Cancer Lett* 2020;473:148–55.
  - 53 Jiang G, Shi L, Zheng X, et al. Androgen receptor affects the response to immune checkpoint therapy by suppressing PD-L1 in hepatocellular carcinoma. *Aging* 2020;12:11466–84.
  - 54 Wang JY, Xiu J, Baca Y, et al. Distinct genomic landscapes of gastroesophageal adenocarcinoma depending on PD-L1 expression identify mutations in Ras-MAPK pathway and TP53 as potential predictors of immunotherapy efficacy. *Ann Oncol* 2021;32:906–16.